

Reprinted from

Infrared Detectors and Focal Plane Arrays III

5–6 April 1994
Orlando, Florida



Volume 2225

Silicide/SiGe Schottky diode infrared detectors

J. R. Jimenez
Electro-Optics Technology Center, Tufts University
Medford, Massachusetts 02155

X. Xiao¹ and J.C. Sturm
Department of Electrical Engineering, Princeton University
Princeton, New Jersey 08544

P.W. Pellegrini and M.M. Weeks
Rome Laboratory
Hanscom Air Force Base, Massachusetts 01731

ABSTRACT

PtSi/Si/SiGe/Si Schottky diode infrared detectors with extended and tunable cut-off wavelengths have been fabricated. Cut-off wavelengths depend on the SiGe composition and extend up to 10 μm for Si₈₀Ge₂₀. The cut-off wavelengths are also tunable by reverse bias. The tunability is due to the SiGe/Si offset serving as an additional potential barrier behind the Schottky barrier that can be varied in energy by a reverse bias. The sensitivity and range of the tunability is controlled by the SiGe thickness and composition. Cut-off wavelengths tunable from 4 μm at zero volts to 10 μm at 3 volts have been obtained. Quantum efficiency values are normal for operation at the long-wavelength end, but reduced over the rest of tunable range, because of the greater distance from the PtSi to the SiGe/Si offset.

1. INTRODUCTION

PtSi/Si Schottky diode detectors are currently in use for infrared imaging at wavelengths below six μm .² This cut-off wavelength is defined by the PtSi/p-Si Schottky barrier height (SBH) of ~ 0.22 eV. For Si-based infrared detectors at longer wavelengths (10-12 μm), several devices have been proposed and are under various stages of development, such as IrSi/Si Schottky diodes^{3,4,5} (SBH ~ 0.12 eV), SiGe/Si heterojunction internal photoemission (HIP) detectors,^{6,7,8} SiGe/Si quantum well infrared photodetectors (QWIPs),^{9,10,11,12} and doping-spike PtSi/Si detectors.¹³ Recently, silicide/SiGe Schottky diodes with extended cut-off wavelengths were demonstrated¹⁴. The diodes were made by reacting Pt with a Si capping layer grown on the SiGe. If the deposited Pt layer is slightly thinner than the Si capping layer, Pt-SiGe reactions, which have been found to result in diodes with higher barrier heights,¹⁵ are avoided. This results, however, in thin layer of unconsumed Si between the PtSi and the SiGe, so that diodes made in this way are more accurately referred to as silicide/Si/SiGe diodes. The unconsumed Si layer forms a thin potential barrier that carriers can tunnel through, lowering the effective Schottky barrier height. In this paper, we report our results on extended cut-off wavelength PtSi/Si/SiGe infrared detectors, and propose and demonstrate silicide/SiGe/Si Schottky diode detectors with voltage-tunable cut-off wavelengths.

2. EXPERIMENTAL DETAILS

The p-type (boron-doped) SiGe structures were grown by rapid-thermal chemical vapor deposition (RTCVD), in a system that has been described previously.¹⁶ The SiGe layers were capped with Si, and a layer of graded Ge concentration was grown between the SiGe and the Si. The Pt depositions were done by electron beam evaporation in a load-locked ultra-high vacuum system. The wafers were RCA-cleaned, which slightly reduces the Si cap thickness and was accounted for in selecting the metal layer thickness. Before deposition, the Si surface was hydrogen-terminated by dipping in aqueous HF solution. The wafers were held at 350 C during deposition and the silicides were formed by annealing in-situ for one hour. For control, silicide/Si diodes were processed and deposited at the same time on boron doped Si substrates (10-15 ohm-cm). Some samples were processed with guard ring structures in the Si below the SiGe. Absolute photoresponse measurements were made with a Perkin-Elmer single-pass monochromator and a SiC globar at 1000 C as the infrared source. The input radiation was chopped at 139 Hz and the photoresponse measured by lock-in amplifier. Measurements were made at a temperature of 40 K or lower, and at various reverse bias voltages.

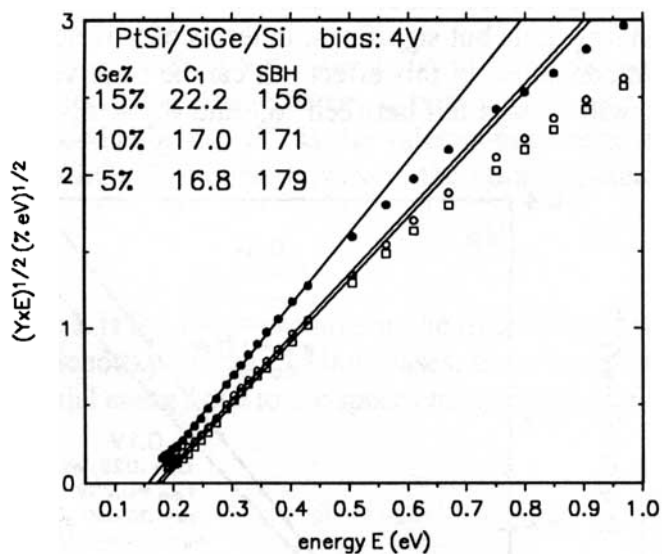


Figure 1: Fowler plots of a series of PtSi/Si/SiGe/Si diodes of varying Ge concentration. Barrier heights are quoted in meV, and the C₁ values are in %/eV.

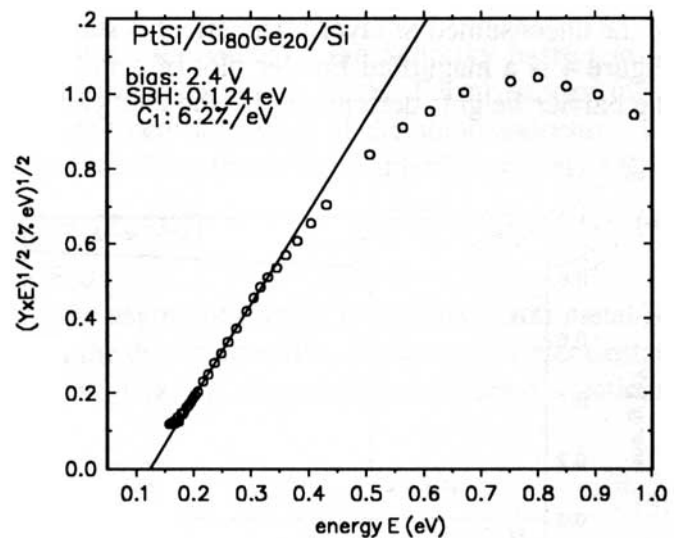


Figure 2: Fowler plot of a PtSi/Si/SiGe/Si diode with 20% Ge. The Schottky barrier height of 124 meV corresponds to a cut-off wavelength of 10 μ m.

3. EXTENDED CUT-OFF WAVELENGTHS

Figures 1 and 2 are Fowler plots of PtSi/Si/SiGe diodes of varying Ge concentration. It can be observed that the extrapolated barrier heights decrease with increasing Ge concentration. This corresponds to an increase in the cut-off wavelengths of the diodes, a significant enhancement of PtSi detector technology. The barrier heights correspond to cut-off wavelengths of 6.8, 7.2, 7.9, and 10 μ m, for 5, 10, 15, and 20 percent Ge, respectively. The basic principle behind such extended-wavelength devices is that the higher valence band energy of SiGe, compared to Si, results in a lower effective barrier for photoexcited holes to surmount. This is illustrated in Figure 3. For diodes made by the reaction of Pt with a Si capping layer, the holes do not "see" the higher PtSi/Si barrier height, but instead tunnel through the barrier formed

by the thin layer of unconsumed Si. Modeling of this tunneling shows that the barrier height extracted in the usual way from photoresponse is always reduced, relative to the PtSi/Si barrier height, by an amount that is less than the SiGe/Si band offset, depending on the Si thickness. In the presence of a tunneling barrier, the equations for internal photoemission are modified to be¹⁵

$$Y = C_1 \tau_{ave} \frac{(h\nu - \phi_{sg})^2}{h\nu} \quad \phi_s > h\nu > \phi_{sg} \quad (1)$$

$$Y = C_1(1 - \tau_{ave}) \frac{(h\nu - \phi_s)^2}{h\nu} + C_1 \tau_{ave} \frac{(h\nu - \phi_{sg})^2}{h\nu} \quad h\nu > \phi_s \quad (2)$$

where C_1 is the emission coefficient in the normal Fowler equation, $h\nu$ is the photon energy, ϕ_s is the PtSi/Si Schottky barrier height, ϕ_{sg} is $\phi_s - \Delta E_v$, where ΔE_v is the SiGe/Si valence band offset, and τ_{ave} is an average tunneling probability for excited carriers with energies between ϕ_{sg} and ϕ_s . The equations predict a change in the slope of the Fowler plot at the PtSi/Si barrier height, which is intuitively expected. The slope below this energy is less than the slope above this energy by an amount that depends on the thickness of the unconsumed Si layer. The effect is small on an energy scale but significant in terms of wavelengths. Figure 4 is a magnified Fowler plot of a PtSi/Si/SiGe diode showing this effect. It can be observed that the barrier height, determined by the energy intercept, will always fall between ϕ_s and $\phi_{sg} = \phi_s - \Delta E_v$.

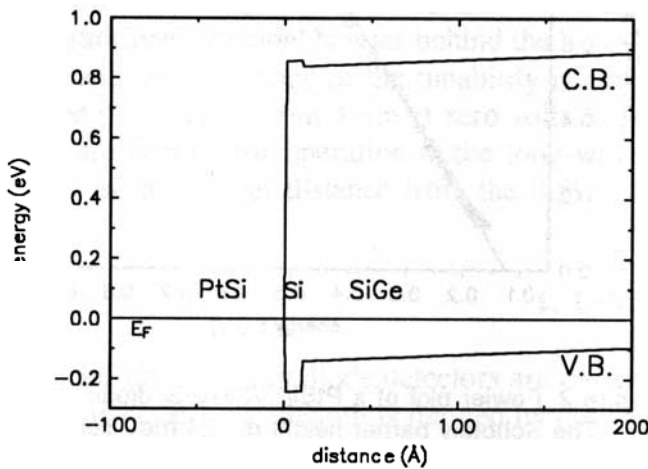


Figure 3: Band diagram of PtSi/Si/SiGe diode showing the relative valence band energies of the SiGe and the Si, and the barrier formed by the Si.

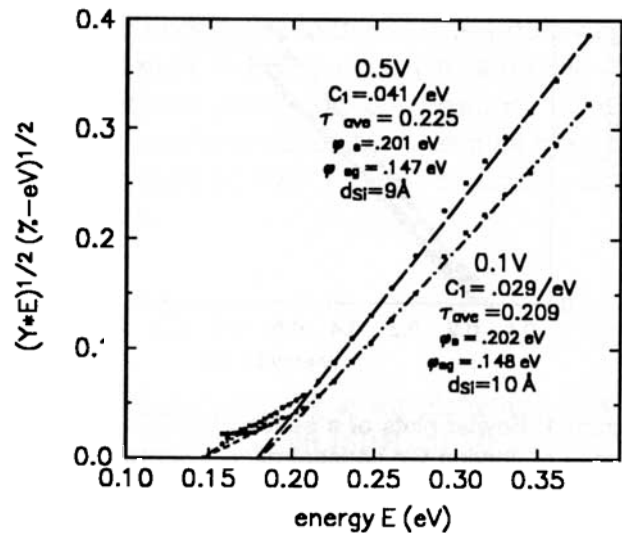


Figure 4: Magnified Fowler plot of a PtSi/Si/SiGe diode (13% Ge), showing the change in slope at low energies due to tunneling through the Si barrier.

The metal-on-Si-cap approach to fabricating Schottky diodes on SiGe is probably not the optimum approach. First of all, it depends on the relative accuracy of two independently measured thicknesses (the Si cap and the metal). Second, the tunneling through the unconsumed Si that inevitably remains reduces the potential quantum efficiency of the device. Third, the variations in the thickness of the unconsumed Si may result in a greater amount of spatial noise over an array. Simultaneous deposition of metal and Si in stoichiometric ratio is a more promising method that would produce an intimate silicide/SiGe interface

without metal-SiGe reactions or an intervening Si layer. The barrier height of the intimate PtSi/Si_{1-x}Ge_x interface, however, is not yet known. This barrier height is not necessarily equal to $\phi_s - \Delta E_v$, as might be expected from an extrapolation of Figure 3 to zero Si thickness. This is because the Schottky barrier height, according to the present understanding, is determined by (among other things) interface states and interface chemistry, which may be sufficiently different for PtSi/Si and PtSi/SiGe interfaces. Studies on such intimate silicide/SiGe interfaces are currently under way.

4. BAND DIAGRAM OF METAL/SiGe/Si DIODES

In this section we calculate the valence band profile of metal/SiGe/Si diodes by modifying the theory of standard Schottky diodes.¹⁷ This is needed to predict the effects of the SiGe/Si-substrate interface. We assume that the SiGe layer is thin enough so that it lies completely in the depletion region. For a given doping and reverse bias, the depletion width is determined by the built-in potential, V_{bi} . For standard diodes, this built in potential is given by¹⁷

$$qV_{bi} = q\phi_{bo} - [E_F - E_v^\infty]$$

where ϕ_{bo} is the asymptotic value of the Schottky barrier, i.e., the value of the Schottky barrier in the absence of the image force, q is the magnitude of the electron charge, E_F is the Fermi energy in the semiconductor and E_v^∞ is the valence band-edge energy in the neutral region of the semiconductor. For metal/SiGe/Si diodes, however, the built in potential is increased by the SiGe/Si interface offset, ΔE_v^x :

$$qV'_{bi} = q\phi_{bo}^x + \Delta E_v^x - [E_F - E_v^\infty] \quad (4)$$

where x is the Ge percentage in the SiGe alloy, and ϕ_{bo}^x is the asymptotic value of the (intimate) metal/Si_{1-x}Ge_x Schottky barrier. In both cases, once V_{bi} is determined, the depletion width, $W(V)$ and the electrostatic potential energy due to the space charge in the depletion region, $U(z, V)$, are given by the known equations¹⁷

$$W(V) = \sqrt{\frac{2\epsilon}{qN_a} \left[V_{bi} + V + \frac{kT}{q} \right]}$$

$$U(z, V) = \frac{q^2 N_a}{\epsilon} \left[W(V)z - \frac{z^2}{2} \right]$$

where N_a is the doping in the SiGe and Si, ϵ is the dielectric constant of Si, T is the absolute temperature, k is Boltzmann's constant, V is the externally applied bias, and z is the distance from the metal-semiconductor interface. The potential energy is referred to a zero of energy at the metal Fermi level. For normal diodes, the valence band-edge energy, $E_v(z)$, is obtained from this electrostatic potential energy by¹⁷

$$E_v(z, V) = -q\phi_{bo} + U(z, V) + \frac{q^2}{16\pi\epsilon_s z} \quad (7)$$

For metal/SiGe/Si diodes, however, instead of adding the Schottky barrier height, we add the initial valence band profile, $E_v^i(z)$ (the valence band-edge energy before any redistribution of charge), which includes the silicide/SiGe Schottky barrier height and the SiGe/Si band offset. Thus

$$E_v(z, V) = E_v^i(z) + U'(z, V) + \frac{q^2}{16\pi\epsilon_s z}$$

If the SiGe layer is of uniform composition throughout its thickness, then the initial valence band profile is

$$E_v^i(z) = \begin{cases} -q\phi_{bo}^x & z < z_{int} \\ -q\phi_{bo}^x - \Delta E_v^x & z > z_{int} \end{cases} \quad (9)$$

where z_{int} is the position of the SiGe/Si interface (i.e., the thickness of the SiGe layer). If the Ge composition is graded, the initial valence band profile changes continuously from $-q\phi_{bo}^x - \Delta E_v^x$ to $-\phi_{bo}^x$. For a PtSi/Si/SiGe/Si diode, the initial valence band profile is

$$E_v^i(z) = \begin{cases} -q\phi_{bo} & z < z'_{int} \\ -q\phi_{bo} + \Delta E_v^x & z'_{int} < z < z_{int} \\ -q\phi_{bo} & z > z_{int} \end{cases}$$

where z'_{int} is the thickness of the unconsumed Si layer. For a PtSi/Si/SiGe/Si diode, the V_{bi} and ϕ_{bo} used are that of Si, not SiGe, assuming that the Si is thick enough that the Schottky barrier height is set by the normal PtSi/Si interface mechanisms. Figure 5 shows typical calculated valence band diagrams, for a PtSi/Si/Si₈₅Ge₁₅/Si diode and a PtSi/Si₈₅Ge₁₅/Si diode. Both diodes have the SiGe/Si interface at 700 Å from the metal, and the last 100 Å of the SiGe is linearly graded in Ge content. For the SiGe/Si offset ΔE_v^x , the empirical dependence of the Si_{1-x}Ge_x bandgap¹⁸ on x was used, together with a 90% - 10% division into valence and conduction band offsets. Except for the Si tunneling barrier, the difference is entirely due to the fact that the $q\phi_{bo}^x$ value used is not equal to $q\phi_{bo}^{Si} - \Delta E_v^x$. This difference has observable effects that will be explained in the next section.

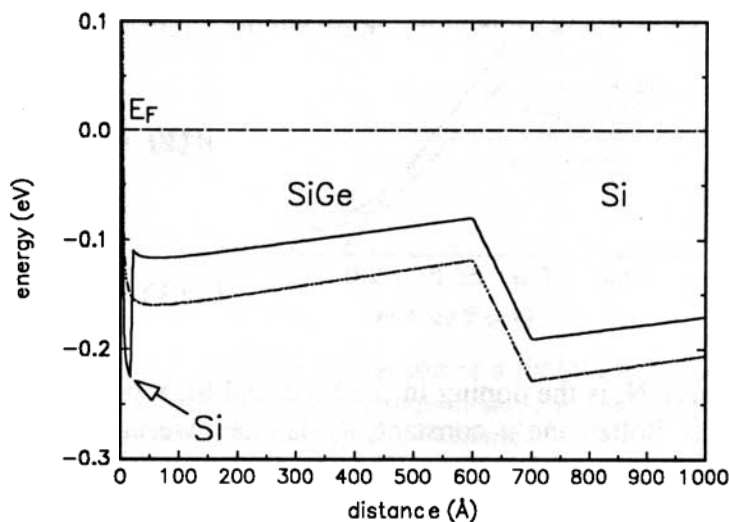


Figure 5: Calculated valence band diagrams of a PtSi/SiGe/Si diode (dotted line) and a PtSi/Si/SiGe/Si diode.

5. VOLTAGE-TUNABLE CUT-OFF WAVELENGTHS

The barrier heights of normal Schottky diodes have a weak dependence on reverse bias voltage. This dependence exists because the image potential causes the maximum of the Schottky barrier to lie inside the semiconductor. The position, z_m , of this maximum is¹⁹

$$z_m(V) = \sqrt{\frac{1}{16\pi N_a W(V)}} \quad (11)$$

and the value of the Schottky barrier at this maximum is¹⁹

$$\phi_b(V) = \phi_{bo} - \frac{q}{2\epsilon_s} \sqrt{\frac{N_a W(V)}{\pi}}$$

For PtSi/Si, the variation is typically of the order of a 10% reduction in the barrier height over a range of 0-30 volts. The reason that this change is so weak is that the position of the Schottky barrier maximum is on the order of about 50 Å, while the externally applied potential difference falls across the whole depletion width, which is typically thousands of angstroms. Figure 6 shows the measured barrier heights as a function of reverse bias of a PtSi/Si control diode and PtSi/Si/SiGe/Si diodes with 5% and 10% Ge, respectively. The variation is typically observed and follows the predictions of equations (10) and (11).

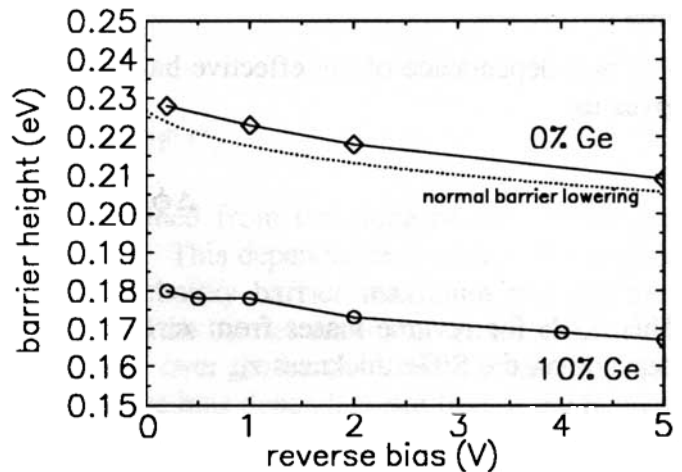


Figure 6: Measured Schottky barrier heights versus bias voltage for PtSi/Si/SiGe/Si diodes with 0% and 10% Ge, respectively.

A much more rapid variation of barrier height with bias is obtained by using the valence band offset at the SiGe/Si interface in conjunction with the Schottky barrier height. If the SiGe layer is thin enough, the SiGe/Si band offset lies just behind the Schottky barrier maximum. Because it starts just slightly below the Schottky barrier (in energy), the band offset forms an additional barrier that extends higher in energy than the Schottky barrier. However, because the offset is deeper in the semiconductor than the Schottky barrier maximum it is much more susceptible to the external bias. It can therefore be lowered in energy by a reverse bias until it is lower in energy than the Schottky barrier. Figures 7 and 8 are calculations of the valence band diagram of PtSi/SiGe/Si diodes at various reverse biases. The structure in Figure 7 has an abrupt SiGe/Si junction, while the structure in Figure 8 has a SiGe layer of the same thickness but graded in composition, showing the possibilities for engineering the barrier profile. For biases such that the SiGe/Si offset peak interface is higher in energy than the Schottky barrier maximum, the effective barrier height, ϕ_{eff} , is simply the value of the valence band energy at the SiGe/Si interface:

$$-q\phi_{eff}(V) = E_v(z_{int}, V)$$

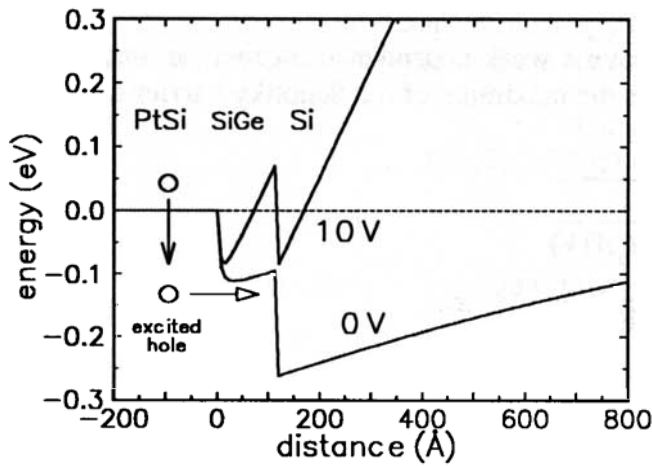


Figure 7: Calculated valence band diagram of a PtSi/Si₈₀Ge₂₀/Si diode with 120 Å of SiGe, at zero and 10 volts reverse bias.

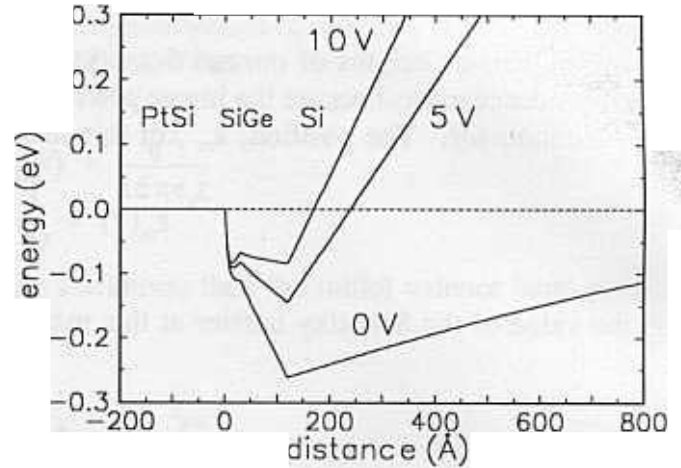


Figure 8: Calculated valence band diagram of a PtSi/SiGe/Si diode at 0, 5, and 10 V reverse bias, with 120 Å of SiGe, linearly graded over 80 Å.

The bias dependence of the effective barrier height, $\Delta\phi_{\text{eff}}(V)$, is therefore $E_v(z_{\text{int}}, V) - E_v(z_{\text{int}}, 0)$. This gives us

$$\Delta\phi_{\text{eff}} = -\frac{q}{\epsilon_s} N_a [W(V) - W(V=0)] z_{\text{int}} \quad (14)$$

This holds for reverse biases from zero up to a bias V such that $\phi_{\text{eff}}(V)$ becomes less than $\phi_b(V)$, and depends on the SiGe thickness z_{int} .

An important point to be noted here is that, in this model, the effective barrier height of PtSi/Si/SiGe/Si diodes can never be higher than the PtSi/Si barrier height, because the increase in the valence band energy at the first Si/SiGe interface is matched by the same decrease at the second SiGe/Si interface. For PtSi/SiGe/Si diodes, however, it may be possible for the effective barrier height to be higher than the PtSi/SiGe/Si barrier height, if the PtSi/SiGe barrier height, $q\phi_{\text{bo}}^x$, is greater than $q\phi_{\text{bo}}^{\text{Si}} - \Delta E_v^x$.

Figure 9 is a series of Fowler plots measured at various reverse bias voltages for a PtSi/Si/SiGe/Si diode with 20% Ge, showing how the barrier heights shift with reverse bias. Figure 10 is a plot of the Schottky barrier heights of PtSi/Si/SiGe/Si diodes with 15% and 20% Ge, respectively. The rapid change of the barrier height, corresponding to emission over the SiGe/Si offset, can be observed, followed by eventual saturation corresponding to emission over the Schottky barrier. The dotted curve is the theoretical reverse bias lowering for a typical PtSi/Si diode. It can be observed that the effective barrier heights at low bias are much higher than the typical PtSi/Si barrier height, which is what would be expected of PtSi/SiGe/Si diodes, and not PtSi/Si/SiGe/Si diodes, in the model above. At present, it is thought that the remaining, interfacial Si layer in these diodes is thin enough so that the Schottky barrier is more characteristic of PtSi/SiGe rather than PtSi/Si. That is, the interfacial Si layer may be so thin (e.g. only a few angstroms), that the interface mechanisms that determine the barrier height are influenced in large part, if not entirely, by the SiGe.

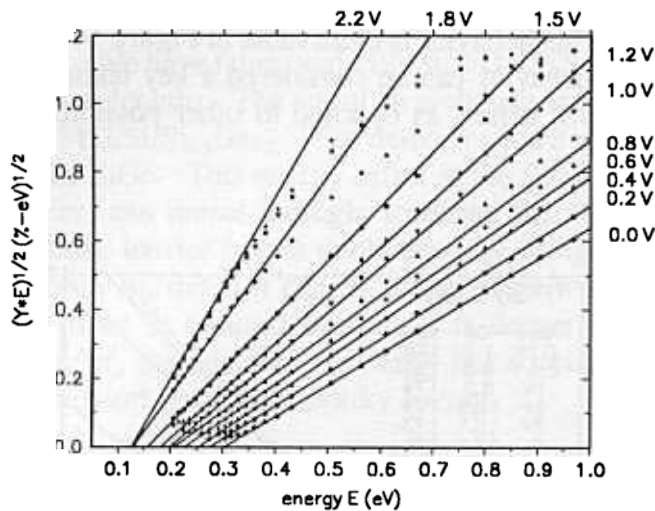


Figure 9: Fowler plots at various reverse biases for a PtSi/Si/SiGe/Si diode, showing how the barrier height shifts with bias.

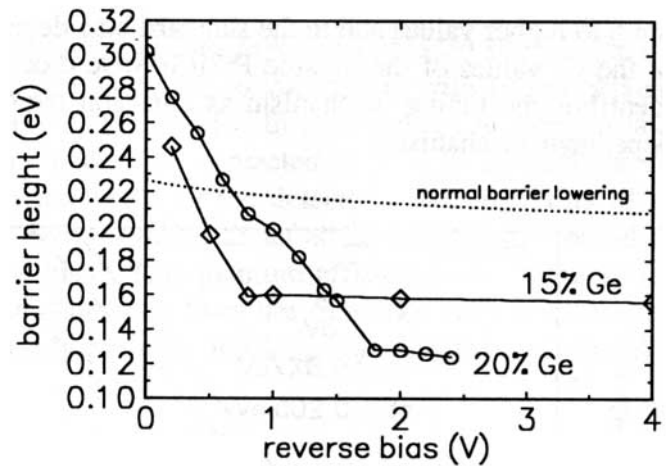


Figure 10: Measured barrier heights as a function of reverse bias for PtSi/Si/SiGe/Si diodes with 15% and 20% Ge.

6. BIAS DEPENDENCE OF C_1

The efficiency coefficient C_1 of PtSi/Si, which is obtained from the slope of the Fowler plot, typically has also a relatively weak dependence on reverse bias. This dependence is understood as being due to scattering in the semiconductor region between the Schottky barrier maximum and the metal interface.¹⁹ The effect of the reverse bias moves the position of the barrier maximum closer to the metal interface. This gives carriers a greater probability of making it over the barrier, and increases C_1 . The dependence is of the form $C_1 \propto \exp(z_m(V)/L)$, where $z_m(V)$ is the bias-dependent position of the Schottky barrier maximum in equation (10), and L is a scattering length in the semiconductor.

The PtSi/Si/SiGe diodes described in this study were found to have a much larger variation of the C_1 coefficient with reverse biases. Figures 11 and 12 are Fowler plots at various bias voltages, showing the typical variation of a PtSi/Si diode, and the much larger variation of the fabricated PtSi/SiGe/Si diodes. This is presumably due to a much smaller scattering length in the epitaxially grown Si and SiGe of the PtSi/Si/SiGe diodes, compared to substrate Si. The scattering length L can be extracted from a linearized plot of C_1 vs. z_m . Figure 13 is a log plot of the emission coefficients C_1 , obtained from the Fowler plots, as a function of the z_m . The peak position z_m is calculated from equation (10). The 10% and 0% samples have the linear behavior typical of Schottky emission, with scattering lengths of $\sim 5 \text{ \AA}$ and $\sim 90 \text{ \AA}$, respectively. The smaller scattering length in the SiGe alloy can be attributed to both alloy scattering and defect scattering in the epitaxially-grown SiGe layer. Defect scattering can be reduced by improved epitaxial control of the SiGe growth process, but alloy scattering is inherent to SiGe.

For tunable PtSi/SiGe/Si diodes, the bias dependence of C_1 is expected to have a distinct characteristic. At lower reverse biases, corresponding to emission over the SiGe/Si offset and rapidly varying effective barrier heights, C_1 values should be low, because the SiGe/Si offset is much further than the Schottky barrier maximum. Furthermore, this C_1 should be relatively voltage-independent, because the peak formed by the SiGe/Si offset does not change position with bias. At some higher reverse bias,

however, when the SiGe/Si offset-peak moves below the Schottky barrier maximum, the C_1 value should jump to higher values and to the standard bias-dependence. This behavior is observable in Figure 14, a plot of the C_1 values of the tunable PtSi/Si/SiGe diodes. Such behavior can be considered a key feature that identifies the tuning mechanism as emission over the SiGe/Si offset, as opposed to other possible bias-dependent mechanisms.

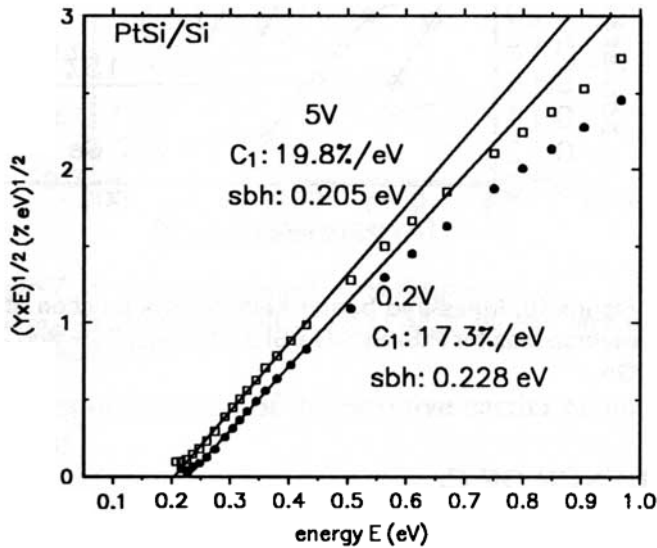


Figure 11: Fowler plots of a PtSi/Si control diode showing a typical variation of the C_1 coefficient (from the slope) with bias.

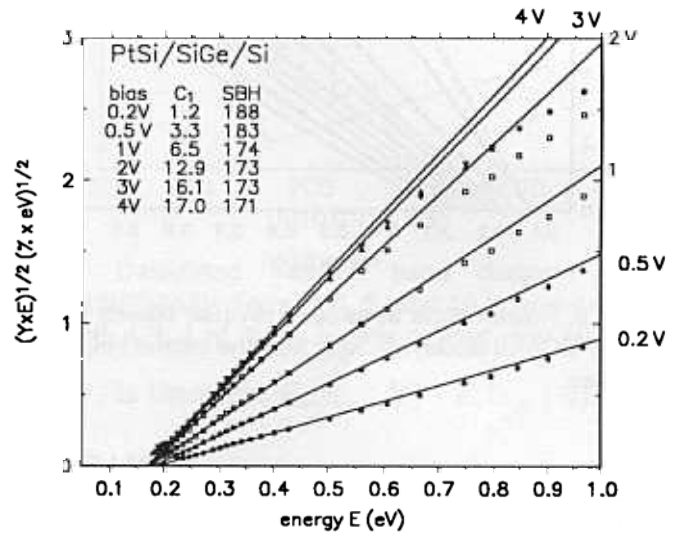


Figure 12: Fowler plots of a PtSi/Si/SiGe/Si diode (with 10% Ge) showing a large variation of the C_1 coefficient with bias.

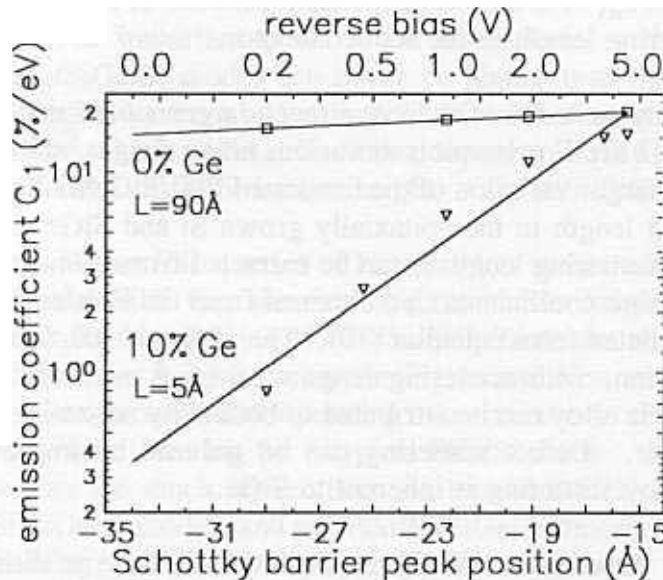


Figure 13: Log plot of the measured C_1 coefficients as a function of the Schottky barrier maximum position showing normal exponential dependence.

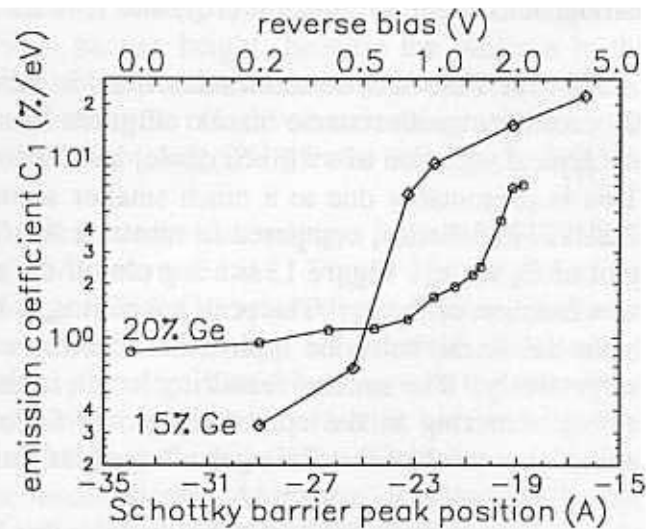


Figure 14: Measured C_1 coefficients for the tunable diodes, versus the bias-dependent Schottky barrier maximum position.

7. SUMMARY

We have fabricated PtSi/Si/SiGe/Si Schottky diode infrared detectors with extended and tunable cut-off wavelengths. The cut-off wavelength increases with increasing Ge concentration, with 10 μm obtained for PtSi/Si/Si_{0.8}Ge_{0.2}. The detectors were made by the reaction of Pt with a pre-grown Si capping layer on the SiGe. This energy offset at the Si/SiGe interface makes the unreacted Si act as a thin barrier that carriers can tunnel through, lowering the effective barrier height of the detector. The tunability of the effective barrier height is obtained by using the other SiGe/Si offset as an additional barrier behind the Schottky barrier that can be pulled down with a reverse bias. The quantum efficiency for emission over this offset is reduced because it is deeper in the semiconductor than the Schottky barrier maximum. However, the quantum efficiency has normal values at larger biases and long-wavelengths corresponding to emission over the Schottky barrier.

ACKNOWLEDGEMENTS

We would like to acknowledge the assistance of James Bockman, helpful discussions with Maxwell M. Chi and Dr. Jonathan Mooney, and the David Sarnoff Research Center for Pt deposition.

REFERENCES

1. Present Address: Intel Corp, MS RN3-21, 2200 Mission College Blvd, Santa Clara, CA 95052
2. F.D. Shepherd, Proc. SPIE 1735, 250 (1992).
3. Paul W. Pellegrini, Aleksandar Golubovic, Charlotte E. Ludington and Melanie M. Weeks, "IrSi Schottky Barrier Diodes for Infrared Detection", IEDM Tech. Digest, 157-160 (1982).
4. Bor-Yeu Tsaur, Melanie M. Weeks, R. Trubiano, Paul W. Pellegrini, and T.R.-Yew, "IrSi Schottky Barrier Infrared Detectors with 10- μm Cutoff Wavelength", IEEE EDL-9, 650-653, (1988).
5. Bor-Yeu Tsaur, Michael J. McNutt, Richard A. Bredthauer, and R.B. Mattson, "128x128-Element IrSi Schottky-Barrier Focal Plane Array", IEEE EDL-10, 361-363 (1989).
6. T.L. Lin and J. Maserjian, "Novel Si_{1-x}Ge_x/Si heterojunction internal photoemission long-wavelength infrared detectors", Appl. Phys. Lett. 57, 1422-1424 (1990).
7. Bor-Yeu Tsaur, C.K. Chen, and S.A. Marino, "Long-Wavelength Ge_xSi_{1-x}/Si Heterojunction Infrared Detectors and 400x400-Element Imager Arrays", IEEE EDL-12, 293-296 (1991).
8. True-Lon Lin, A. Ksendzov, Suzan M. Dejewski, Eric W. Jones, Robert W. Fathauer, Timothy N. Krabach, and Joseph Maserjian, "SiGe/Si Heterojunction Internal Photoemission Long-Wavelength Infrared Detectors Fabricated by Molecular Beam Epitaxy", IEEE Trans. El. Dev. 38, 1141-1144 (1991).

9. R.P.G. Karunasiri, J.S. Park, and K.L. Wang, "Si_{1-x}Ge_x/Si multiple quantum well infrared detector", *Appl. Phys. Lett.* 59, 2588-2590 (1991).
10. J.S. Park, R.P.G. Karunasiri, and K.L. Wang, "Normal incidence infrared detector using p-type SiGe/Si multiple quantum wells", *Appl. Phys. Lett.* 60, 103-105 (1991).
11. R. People, J.C. Bean, C.G. Bethea, S.K. Sputz, and L.J. Peticolas, "Broadband (8-14 μ m), normal incidence, pseudomorphic Ge_xSi_{1-x}/Si strained-layer infrared photodetector operating between 20 and 77 K", *Appl. Phys. Lett.* 61, 1122-1124 (1992).
12. R.P.G. Karunasiri, J.S. Park, and K.L. Wang, "Normal-incidence infrared detector using intervalence-subband transitions in Si_{1-x}Ge_x/Si quantum wells", *Appl. Phys. Lett.* 61, 2434-2436 (1992).
13. T.L. Lin, J.S. Park, T. George, E.W. Jones, R.W. Fathauer, and J. Maserjian, "Long-Wavelength PtSi infrared detectors fabricated by incorporating a p⁺ doping spike grown by molecular beam epitaxy", *Appl. Phys. Lett.* 62, 3318-3320 (1993).
14. X. Xiao, J.C. Sturm, S.R. Parihar, S.A. Lyon, D. Meyerhofer, S. Palfrey, and F.V. Shallcross, "Silicide/SiGe Schottky Diode Infrared Detectors", *IEEE EDL-14*, 199 (1993).
15. J.R. Jimenez, X. Xiao, J.C. Sturm, P.W. Pellegrini, and M.M. Weeks, "Schottky barrier heights of Pt and Ir silicides formed on Si/SiGe measured by internal photoemission" *J. Appl. Phys.* 75, 1994 (to be published).
16. J.C. Sturm, P.V. Schwartz, E.J. Prinz, and H. Manoharan, "Growth of SiGe by rapid thermal chemical vapor deposition and application to heterojunction bipolar transistors", *J. Vac. Sci. Technol. B* 9, 201-2016 (1991).
17. S. M. Sze, "Physics of Semiconductor Devices", Wiley, New York 1981, Chapter 5.
18. John C. Bean, "Silicon-Based Semiconductor Heterostructures: Column IV Bandgap Engineering", *Proc. IEEE*, 80 p. 571-587 (1992).
19. J.M. Mooney, "The dependence of the Schottky emission coefficient on reverse bias", *J. Appl. Phys.* 65, 2869-2872 (1989).